MEASURING THE ANGULAR DISTRIBUTIONS OF 14.1 MEV NEUTRONS SCATTERING ON CARBON NUCLEI

D.N. Grozdanov on behalf of TANGRA collaboration
dimitar@nf.jinr.ru

Outline

- Project «TANGRA»
- Motivation and object of research
- Experimental setup
- Measurement of “tagged” neutron beam profiles
- Cross-section equation
- Intrinsic efficiency of the neutron detector
- Solid angle calculation
- Experimental data processing
- Angular distributions of scattered neutrons
- Conclusions

TANGRA project

Project «**TANGRA**» (**TA**gged **N**eutron and **G**amma **RA**ys) at JINR-FLNP (Dubna) is aimed at studying nuclear reactions induced by fast neutrons. At a TANGRA setup, the sample under investigation is irradiated with 14-MeV neutrons, produced by the ING-27 neutron generator.

- The main feature of the setup is the use of the **tagged neutron method (TNM)**.
- Basically, the angular distributions of γ-rays and partial cross sections of detected γ-transitions were measured [1-3].
- Recently, the angular distributions of scattered neutrons have been measured.

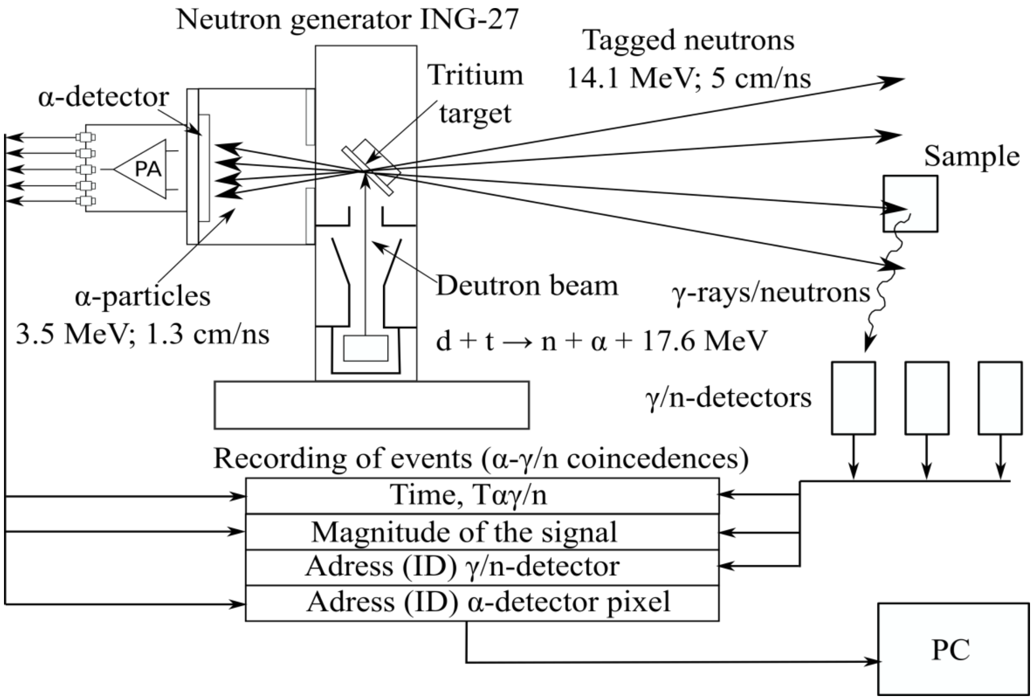

Fig. 1. Standard diagram of TANGRA experimental setups.

1. N.A. Fedorov *et al.* Bull. Russ. Acad. Sci.: Phys. **84** (2020) 367
2. D.N. Grozdanov *et al.* Phys. At. Nucl. **81** (2018) 588
3. D.N. Grozdanov *et al.* Phys. At. Nucl. **83** (2020) 384

Motivation and the object of research

Object of our research – ^{12}C nuclei.

- This is a light nucleus with a relatively high energy of the first excited state (4.44 MeV), which decays with the emission of n- and γ- radiation.
- The second and the third excited states are decaying through α-particle breakup.
- First excited states can be treated in the collective model [4, 5] using the rotational approach for a strongly oblate nucleus.

Table 1. Quadrupole deformation β_2 for ^{12}C state obtained from various sources using different methods.

$\beta_2(B(E2)\uparrow)$	$\beta_2(Q_{mom})$	β_2 (OM, CC)	β_2 (OM, CC)
0.592 ± 0.036 [6]	-0.411 ± 0.226 [7]	-0.62 [4]	-0.60 [5]

4. Z.M. Chen *et al.* J. Phys. G: Nucl. Part. Phys. **19** (1993) 877
5. G.A. Grin *et al.* Phys. Lett. **25B** (1967) 387
6. S. Raman *et al.* At. Data Nucl. Data Tables **78** (2001) 1
7. W.J. Vermeer *et al.* Phys.Lett. **122B** (1983) 23

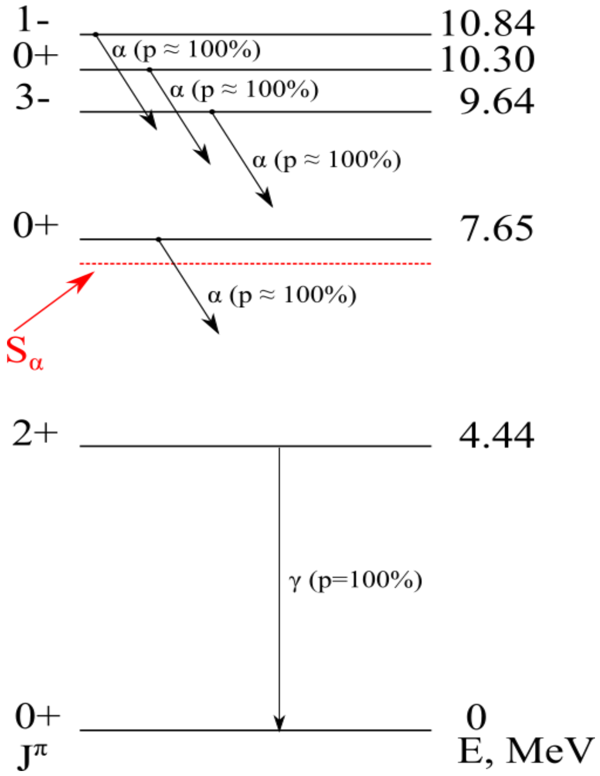

Fig. 2. Scheme for ^{12}C low-lying levels with the de-excitation processes probabilities *p*. S_α stands for α-particle separation energy.

Experimental setup

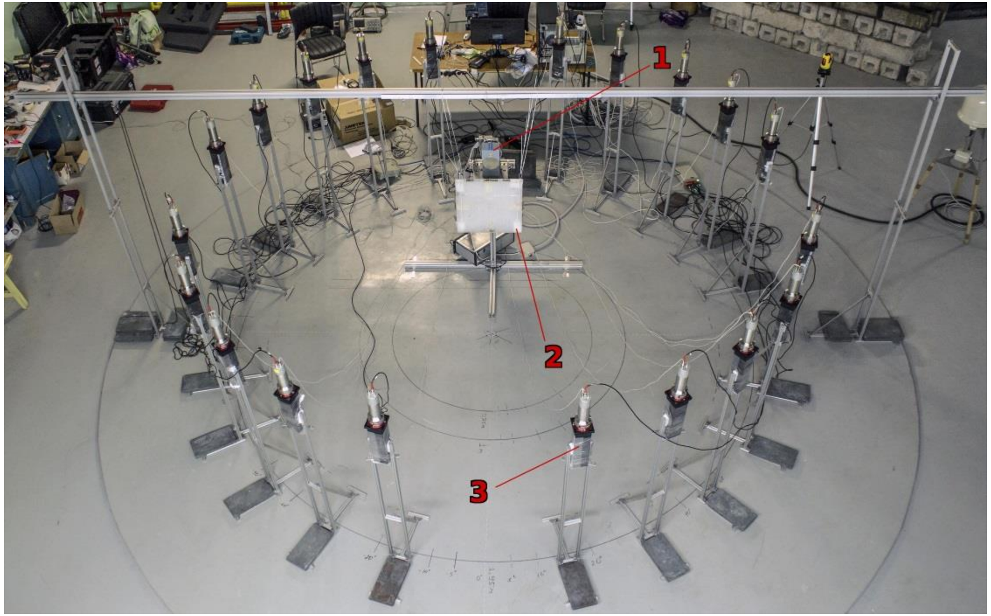

Fig. 3. Photo of the TANGRA setup with plastic detectors for measuring angular distributions of the scattered neutrons. *1* – ING-27 neutron generator, *2* – irradiated carbon sample, *3* – one of the 20 plastic detectors used in the registration system.

Neutron source: ING-27 generator

Sample: graphite block, 44 cm x 44 cm x 2 cm

Neutron detector: polyphenyltoluene detector ($Z \approx 5.5$)

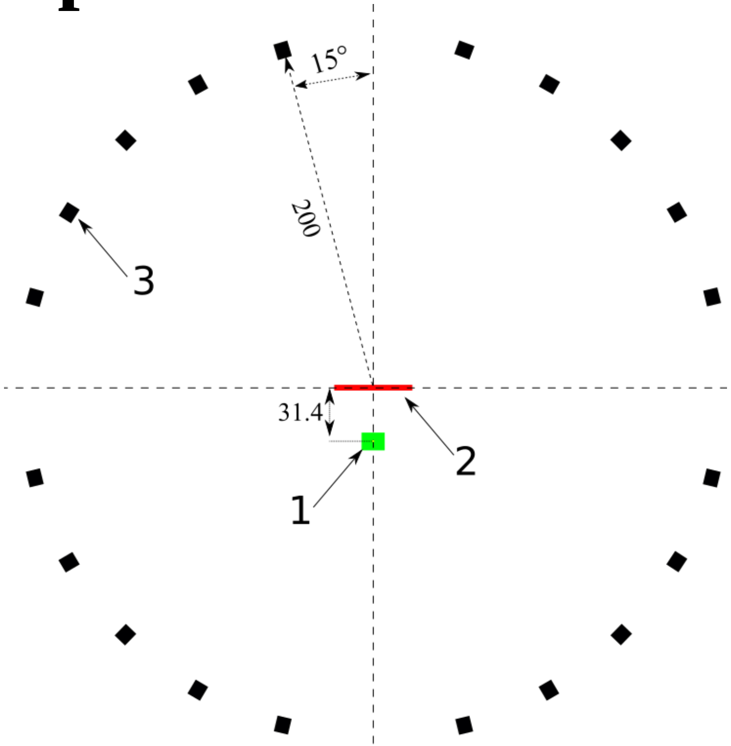

Fig. 4. Scheme of the TANGRA setup with plastic detectors for measuring angular distributions of the scattered neutrons. Designations as in Fig. 3. Dimensions are in cm.

ING-27

Neutron detector

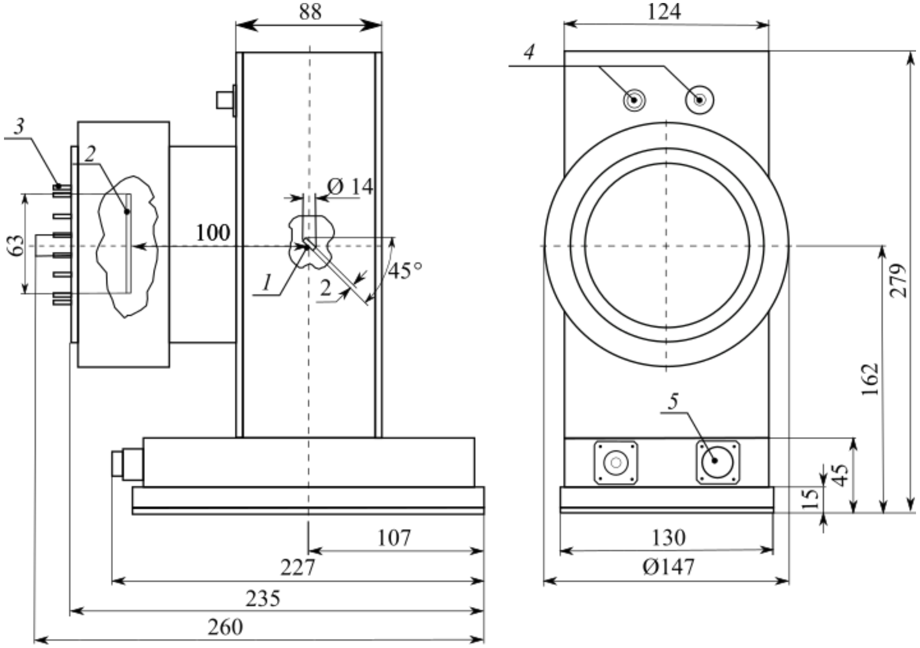

Fig. 5. 1 – neutron generator target, 2 – α-detector, 3 – signal connector of α-detector, 4 – high-voltage power connectors, 5 - low-voltage control connector

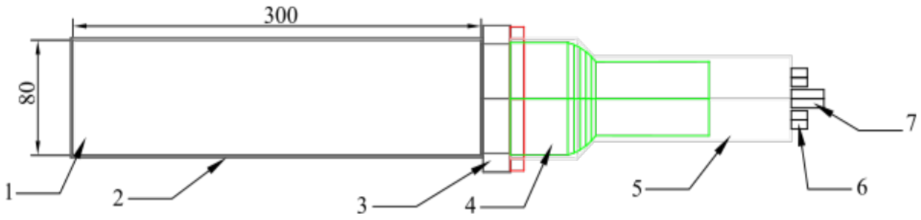

Fig. 6. 1 - plastic scintillator, 2 - reflective winding, 3 - aluminium holder, 4 - ETL9821KFLB photomultiplier, 5 - magnetic screen, 6 - BNC connectors (x2) and 7 - SHV connector.

Measurement of “tagged” neutron beam profiles

2D-detector, made of 4 double-sided stripped position-sensitive Si-detectors

Each Si detector consists of 32 x 32 strips
~1.8 mm thick
Size of one detector: 60x60 mm^2
Total size: 120x120 mm^2
Thickness: 0.3 mm
Neutron detection efficiency: ~ 0.8%
Each 8 strips are grouped together, forming a matrix 8x8 with a pixel size of ~1.5x1.5 cm^2

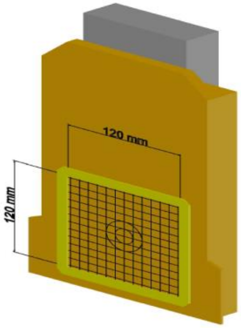

Fig. 7. Schematic illustration of the 2D detector

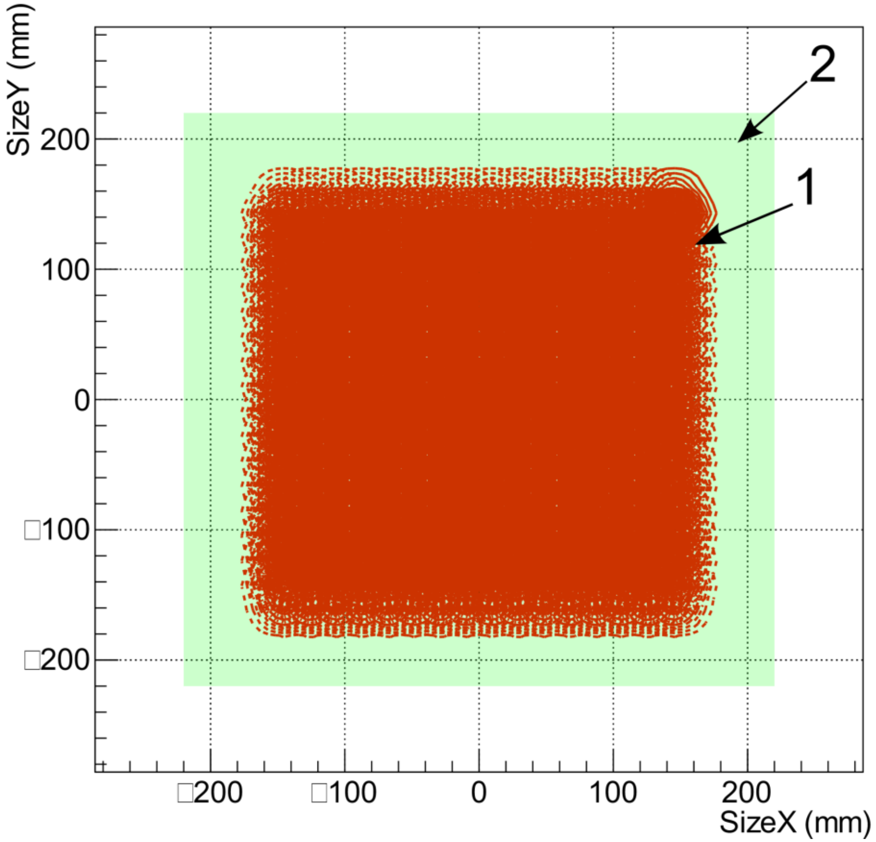

Fig. 8. Neutron beam 2D profile (1) on the target (2).

Cross-section equation

$$\left(\frac{d\sigma}{d\Omega}\right)_\theta = \frac{N(\theta)}{N_\alpha C N_{nucl}} \cos(\psi) \times 10^{27} \left[\frac{mb}{sr}\right], C = \epsilon d\Omega, N_{nucl} = \frac{\rho N_a D}{A}$$

Where:

θ - is the angle between the beam and the direction towards the detector from the point of interaction of the beam with the target

N(θ) - count of the neutron detector for the angle θ in coincidence with the X strip of the alpha detector

N_α - Neutron counting (alpha detector count without coincidence)

C - correction factor

ϵ - neutron detector intrinsic efficiency

$d\Omega$ - solid angle covered by a neutron detector [1/sr]

N_{nucl} - average number of nuclei

A - mass number of target atoms = 12 [g/mol]

ρ - target density = 1.6405 [g/cm^3]

N_a - Avogadro's number = 6.02 x 10^{23} [1/mol]

D - target thickness = 2 [cm]

$\cos(\psi)$ - angle between beam and axis of symmetry

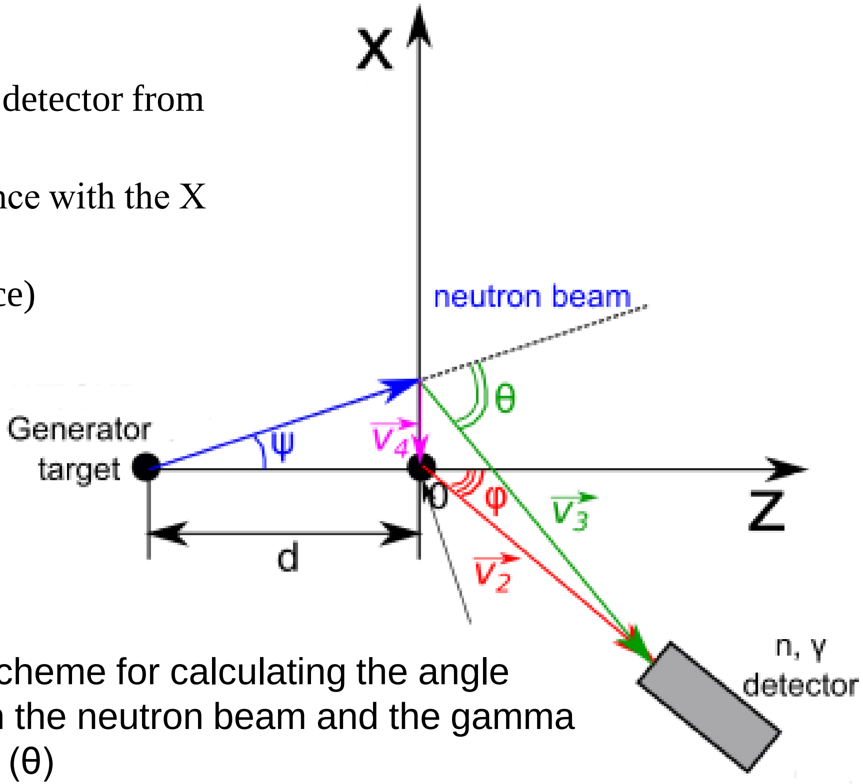

Fig. 9. Scheme for calculating the angle between the neutron beam and the gamma detector (θ)

Intrinsic efficiency of the neutron detector

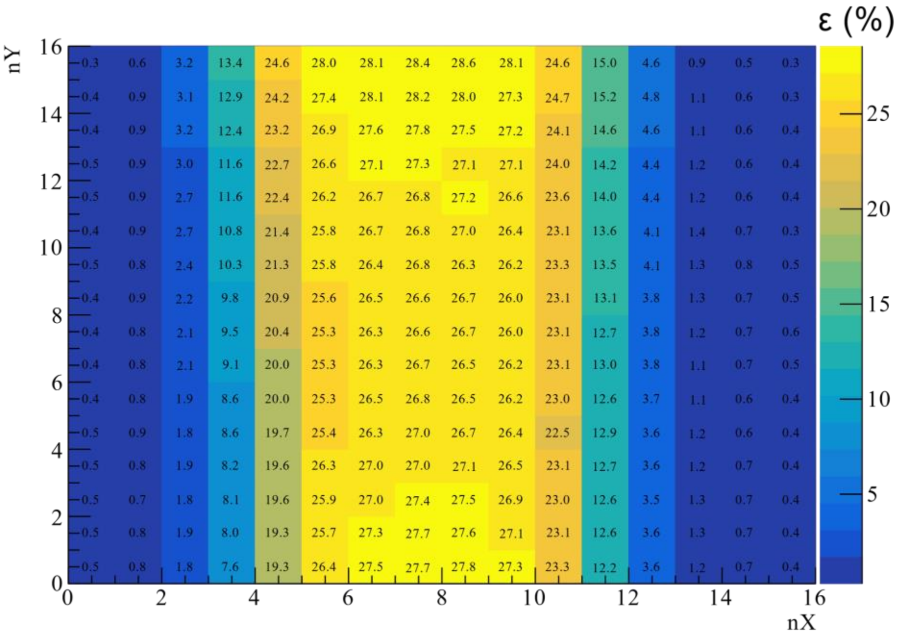

Fig. 10. Experimental intrinsic efficiency ϵ (%) for 14.1 (MeV) neutrons for one detector

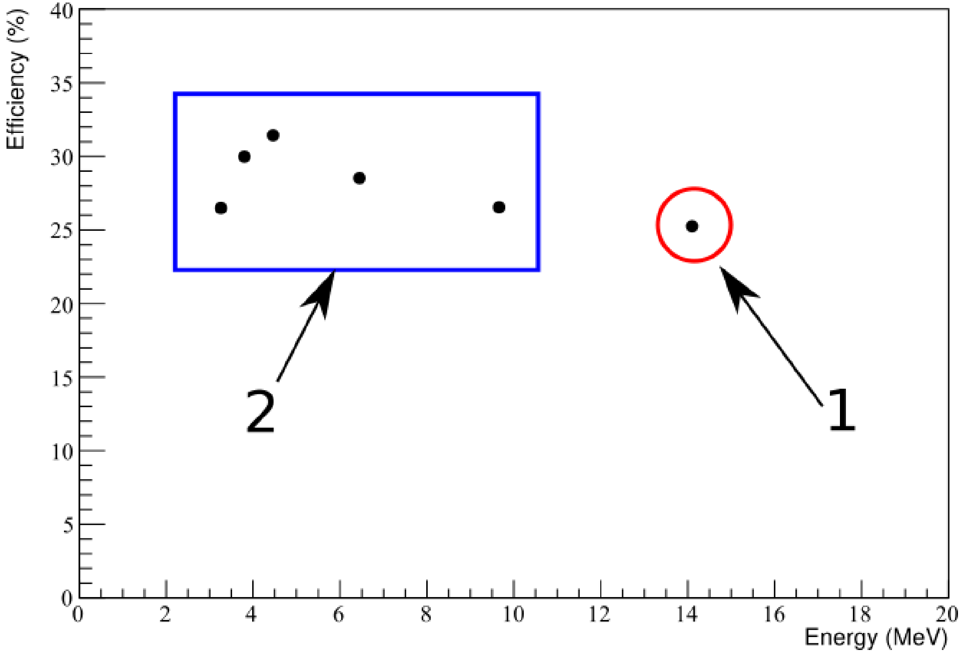

Fig. 11. Geant4 intrinsic efficiency ϵ (%) for neutrons with different energy. Where: 1 – is experimental measurement and 2 – modeling.

Solid angle calculation

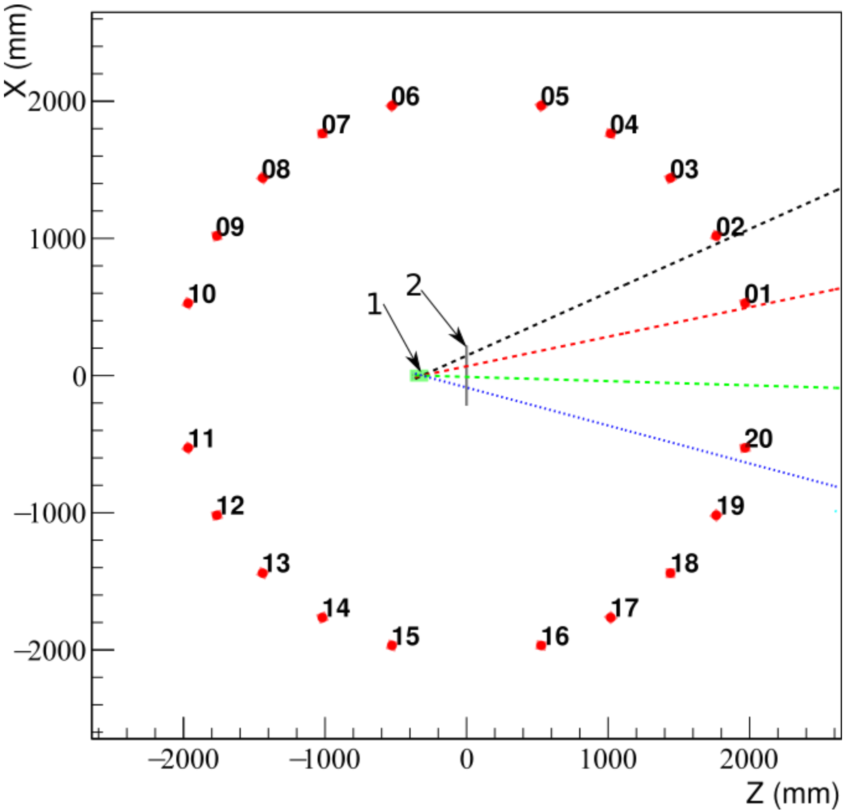

Fig. 8. Scheme of the TANGRA setup with some of “tagged” neutron beam’s. Where: 1 – is ING-27, 2 – target.

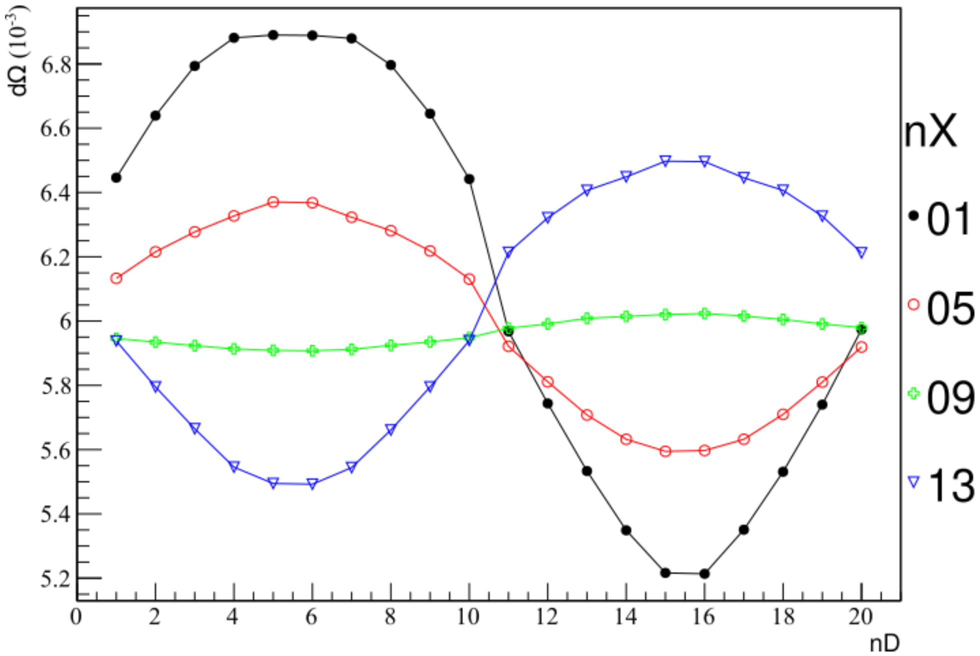

Fig. 13. Geant4 solid angle calculation.

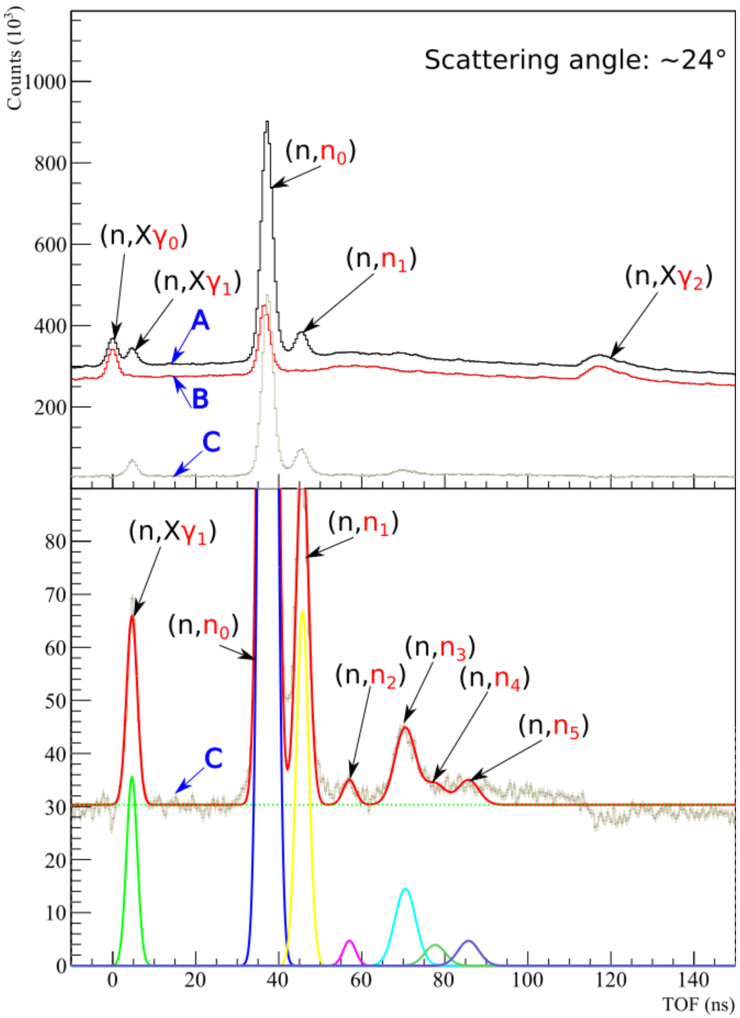

Experimental data processing

Fig. 14. Examples of the time-of-flight spectra obtained. Peaks are labelled with source reaction, registered particle is painted red.
Where:

A – is measurement with target (^{12}C), Time ~ 48h;

B – is measurement without target (Background), Time ~ 28h,

C – Net spectra (without background)

$(n,X\gamma_0)$ – γ from ING-27

$(n,X\gamma_1)$ – γ from target (^{12}C)

$(n,X\gamma_2)$ – γ from the opposite wall

(n,n_0) - elastic scattering

(n,n_1) - inelastic scattering to the 1 excited state of ^{12}C 4.44MeV

(n,n_2) - inelastic scattering to the 2 excited state of ^{12}C 7.65MeV

(n,n_3) - inelastic scattering to the 3 excited state of ^{12}C 9.64MeV

(n,n_4) - inelastic scattering to the 4 excited state of ^{12}C 10.30MeV

(n,n_5) - inelastic scattering to the 5 excited state of ^{12}C 10.84MeV

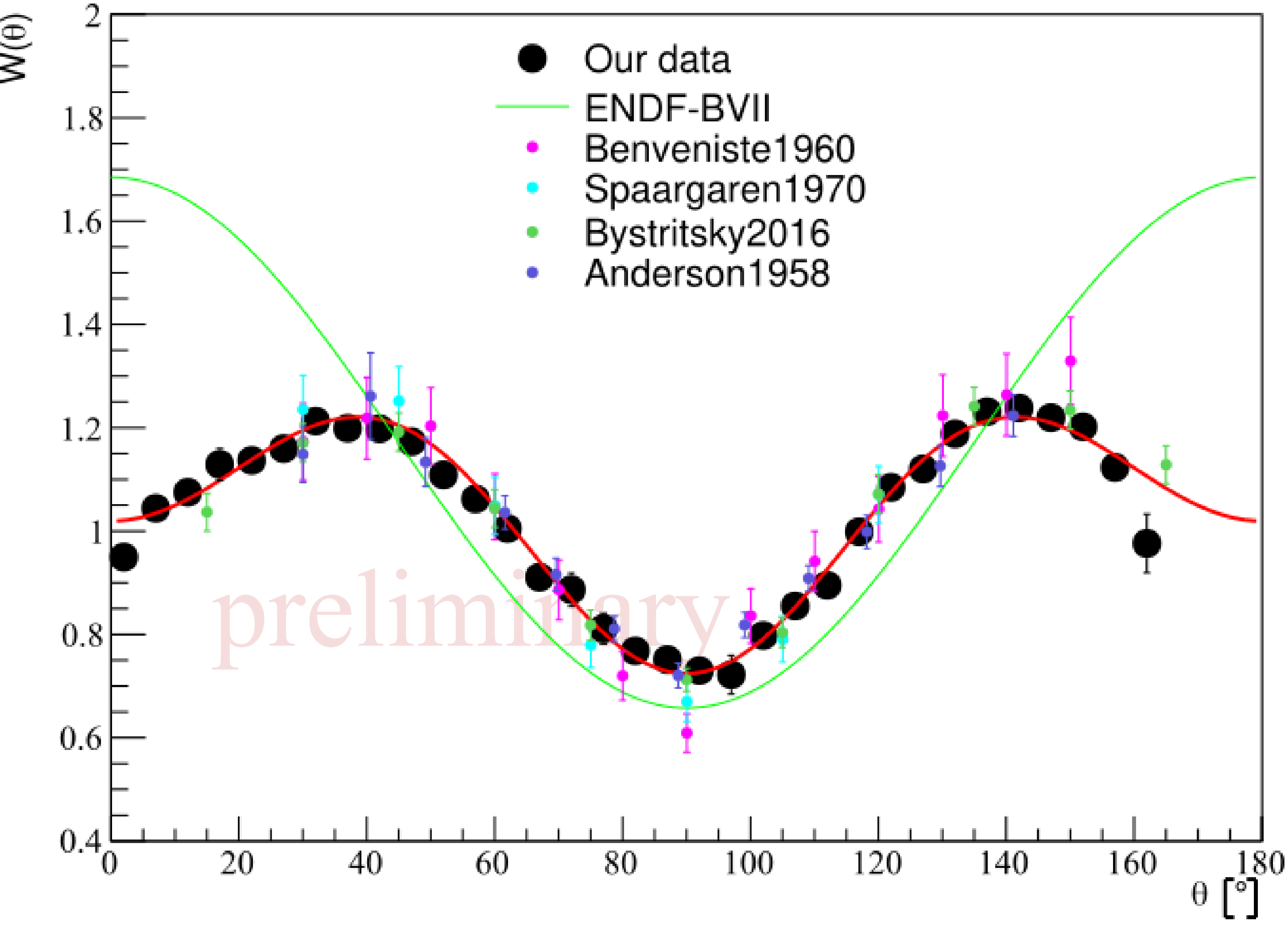

Fig.15. Angular anisotropy of 4.43-MeV γ-rays produced in inelastic scattering of 14.1-MeV neutrons by 12C nuclei

$$W(\theta) = 1 + \sum_{I=2,4\ldots}^{2J} a_I P_I(\cos\theta)$$

Source	a_2	a_4
Our data	0.32 (0.01)	-0.30 (0.01)
Bystrirsky	0.34 (0.02)	-0.33 (0.02)
Anderson	0.29 (0.22)	-0.28 (0.02)
Benveniste	0.37 (0.05)	-0.39 (0.7)
Spaargaren	0.39 (0.01)	-0.37 (0.01)
ENDF/B-VIII	0.68	

Angular distributions of scattered neutrons

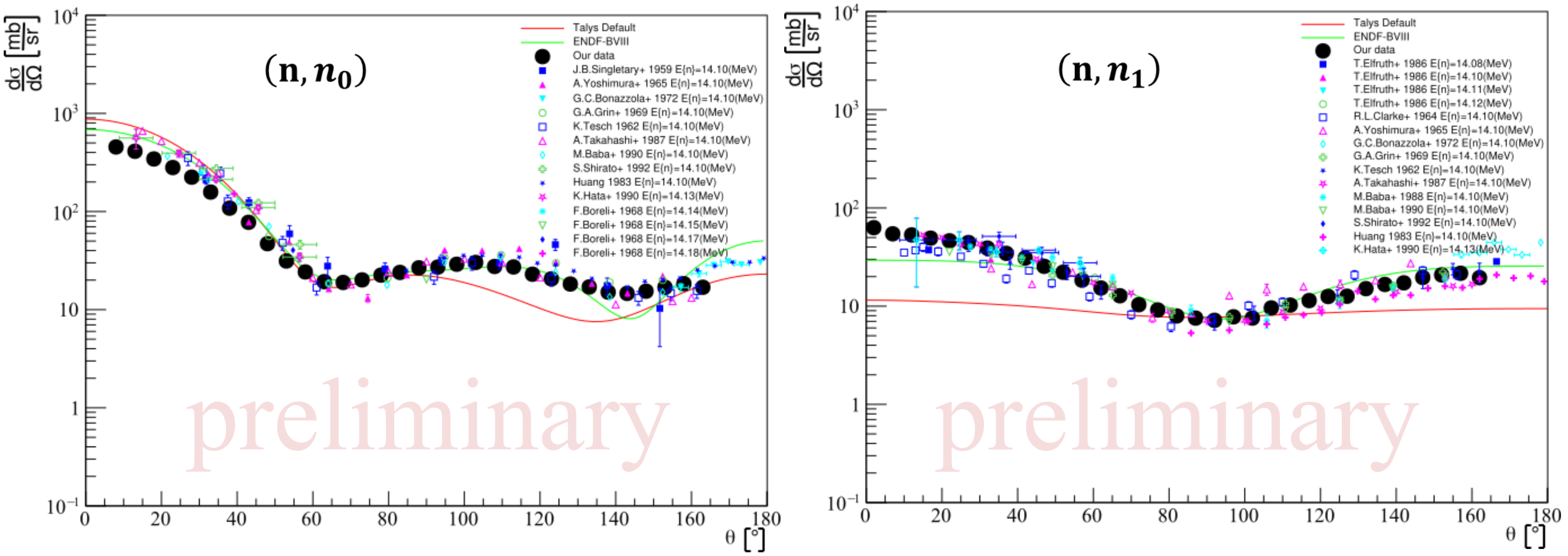

Fig.16. Differential cross sections for neutron scattering on **^{12}C**
in comparison with experimental data.

Angular distributions of scattered neutrons

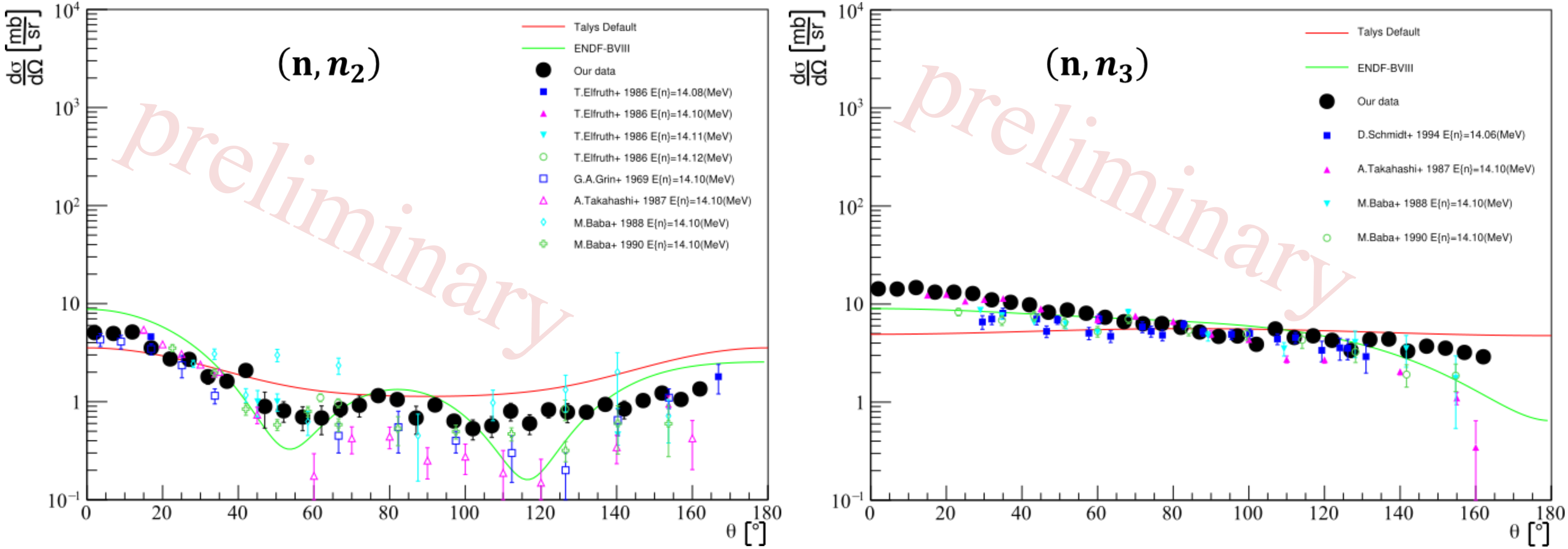

Fig.17. Differential cross sections for neutron scattering on ^{12}C in comparison with experimental data.

Angular distributions of scattered neutrons

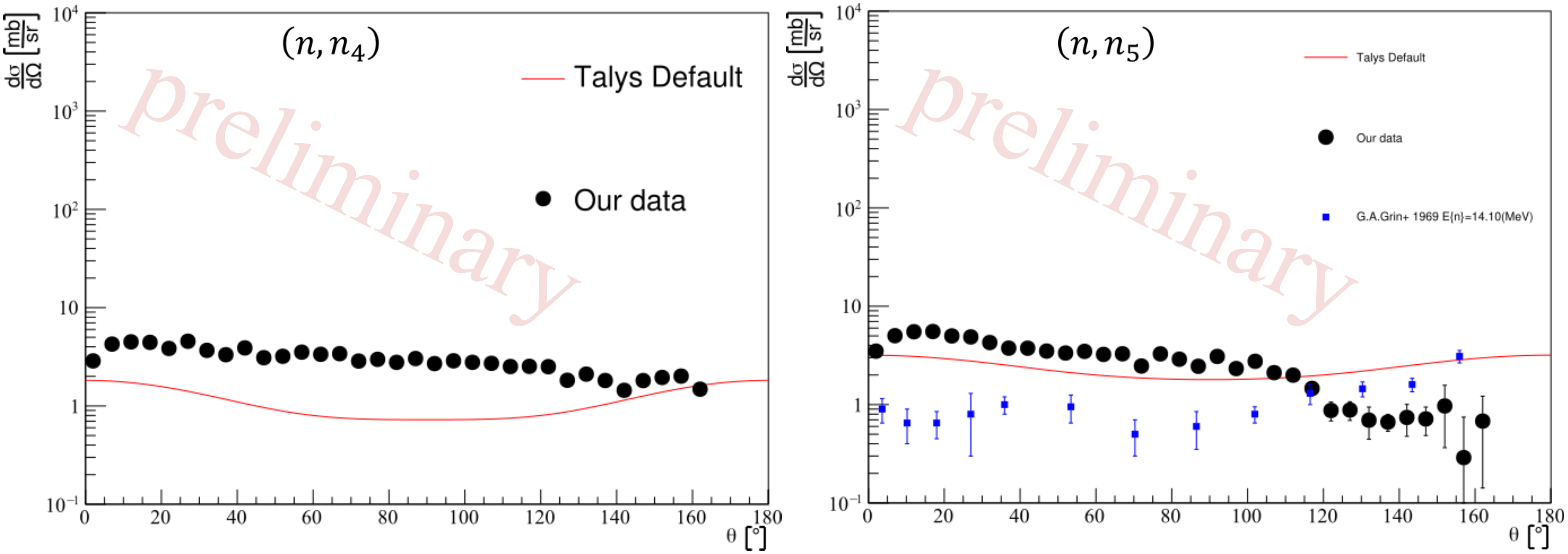

Fig.18. Differential cross sections for neutron scattering on ^{12}C in comparison with experimental data.

Conclusions

As a result of the work:

- Experiment of neutron scattering on carbon carried out by TANGRA setup showed us possibility to measure angular distributions of scattered neutrons and even, with some improvements, differential cross sections of scattered neutrons.
- It was confirmed that the experimental technique used in this work is capable of studying the up to five excited states of ^{12}C.
- Showing good agreement between our data and other work, the angular distribution for the fourth excited states of ^{12}C was measured for the first time.

Thank you for your attention

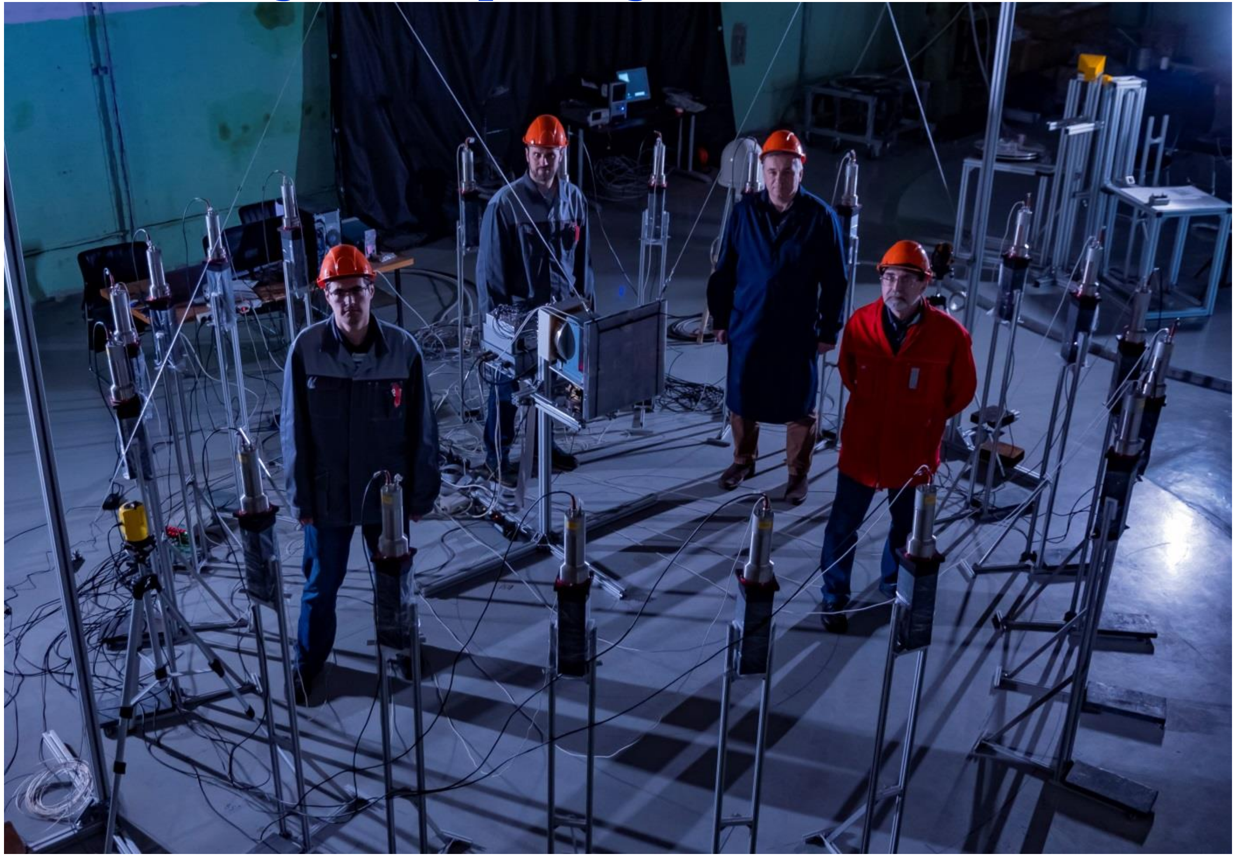

Good team @ Good results

TALYS nuclear reaction code

TALYS is a code for nuclear reaction calculations. It covers an extensive range of projectile energies (1 keV – 200 MeV) and nuclei masses (A ≥ 12).

TALYS has implementations of several models for nuclear reaction description: for direct processes (DWBA, CC), compound-nucleus processes (Hauser-Feshbach models), nuclear level densities (Fermi-gas model and others).

TALYS 1.9 was used for calculation of:

•Partial γ-transitions cross sections

•Differential cross sections of elastic and inelastic neutron scattering

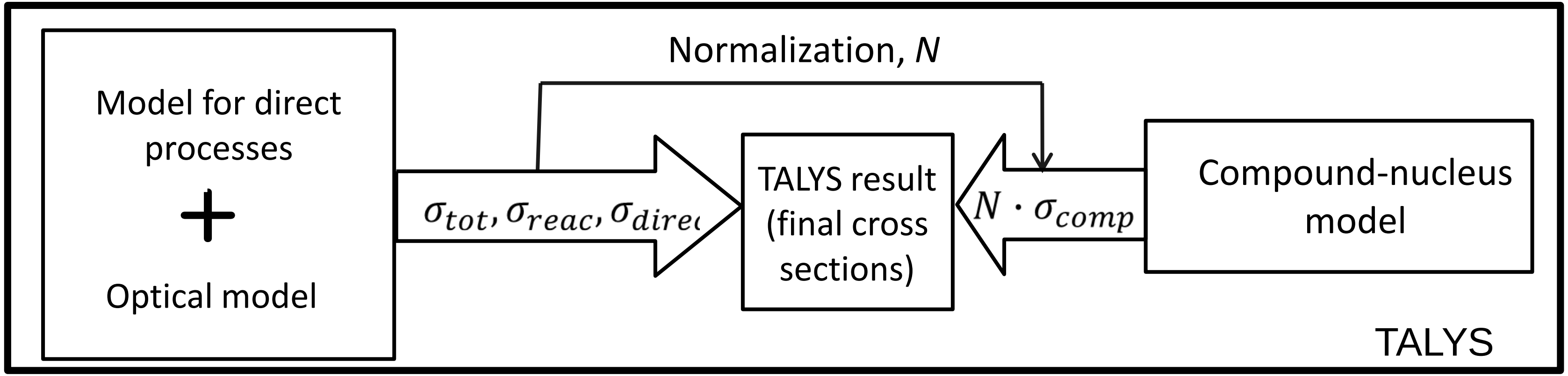

Fig.7. Scheme of the complementary use of nuclear models in the TALYS 1.9 calculations.

Approximation procedure

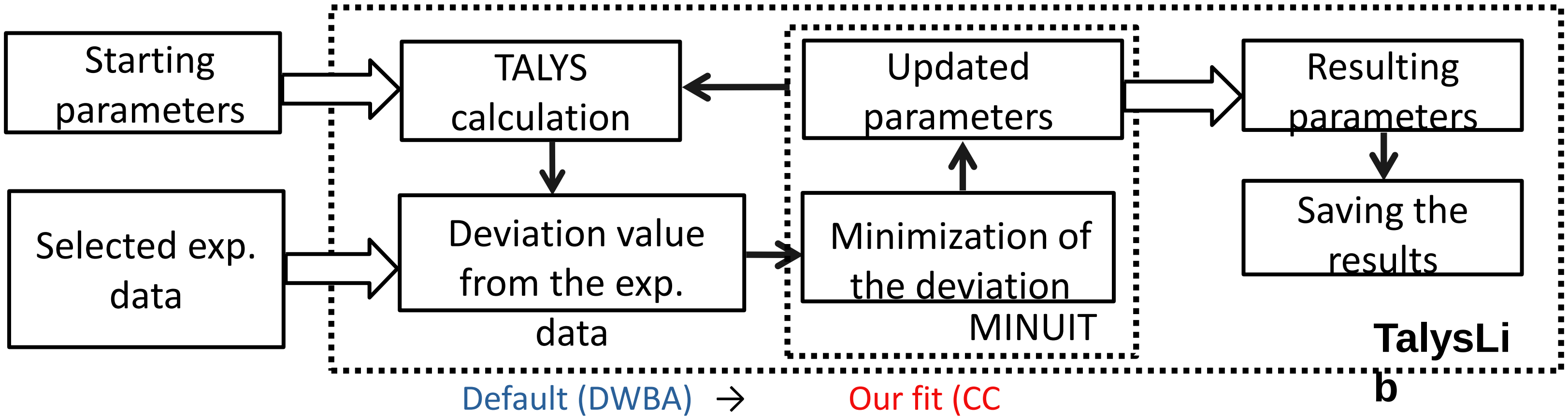

Default (DWBA) → Our fit (CC rotational)

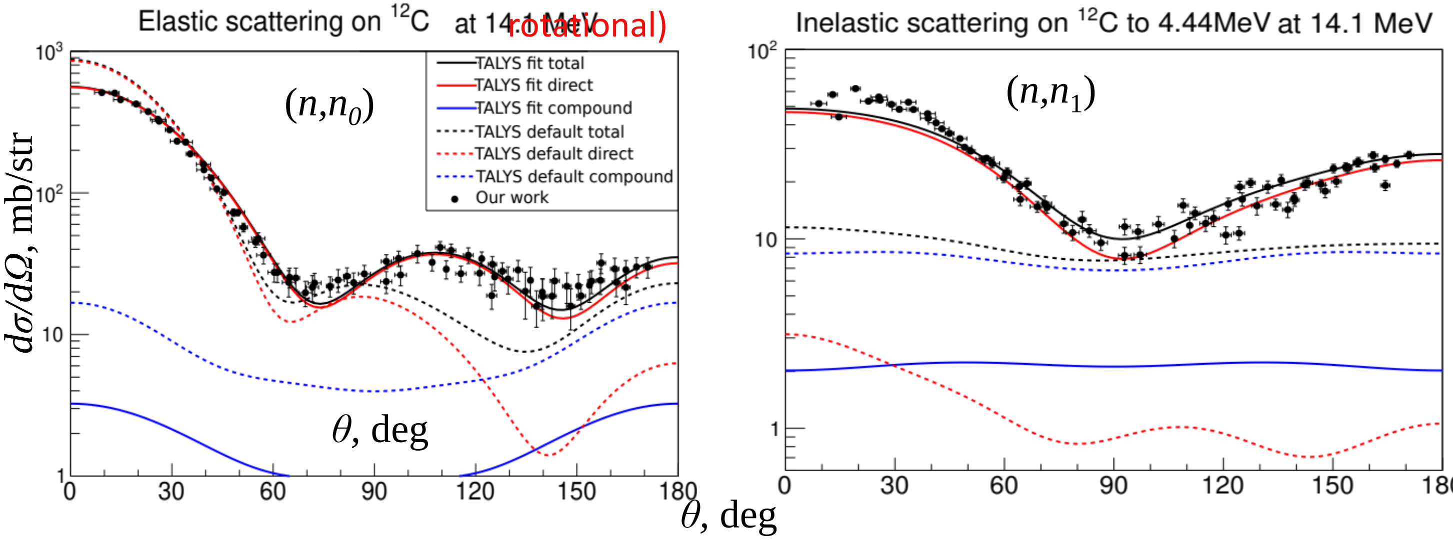

Fig.8. Differential cross section approximation in TalysLib for ^{12}C based on our experimental data.

Annex: TALYS 1.9: **Optical parameters for 14.1 MeV**

Source	Approach	V_V MeV	W_V MeV	r_V fm	a_V fm	W_D MeV	r_D fm	a_D fm	V_{SO} MeV	W_{SO} MeV	r_{SO} fm	a_{SO} fm	β_2	χ^2/N
Default calc.	DWBA	49.07	1.26	1.13	0.68	7.65	1.31	0.54	5.39	-0.07	0.90	0.59	0.40	73.5
Our data fit	CC rot.	49.78	0.03	1.05	0.51	3.74	1.27	0.31	7.79	-3.38	1.00	0.55	-0.95	2.49
Other data fit	CC rot.	49.73	0.21	1.11	0.44	5.42	1.20	0.34	6.31	-3.75	1.21	0.59	-0.83	2.72

(*N* stands for number of experimental points used in the fit. The notations in the tables are the same as in the optical model parametrization of A.J. Koning and J.P. Delaroche [12].)

Comparison of integral cross sections of several processes taking place at 14.1 MeV

	σ_{tot} mb	Σ_{inl} mb	σ_{el} mb	$\sigma(n,n_1)$ mb	$\sigma(n,n_2)$ mb	$\sigma(n,n_3)$ mb	$\sigma_\gamma(2_1^+ \rightarrow 0_{g.s.}^+)$ mb
Experiment	1290±100[13] 1430±100[14]	1,05	784±45[9]	203±12[9]	11±1[9]	63±4[5]	180±7[15] 168±20[16]
Default calc.	1572	341	866	142	19	68	202
Our data fit	1241	311	829	263	6	11	279
Other data fit	1264	293	826	211	8	22	237

[12] A.J. Koning and J.P. Delaroche, Nucl.Phys.A **713** (2003) 231. [13] M.J.Rapp *et al*. Nucl. Sci.Eng. **172** (2012) 268. [14] S.V.Artemov *et al*. Bull. Russ. Acad. Sci.: Phys. 84 (2020) 894. [15] I.Murata *et al.* Conf.on Nucl.Data For Sci.and Technol., Mito (1988) 275. [16] V.C.Rogers *et al.* Nucl. Sci Eng. **58** (1975) 298

Annex: Optical model potential

It is believed that the interaction between the neutron and the nucleus can be described by the complex potential.
Real part takes account of the refraction of particle wave on the nucleus border.
Imaginary part takes account of wave absorption as such, all of the nonelastic reactions.
Optical model cannot describe inelastic channels of nuclear reaction separately without some modifications.

The default optical model potentials used in TALYS are the local and global parametrisations of Koning and Delaroche [12]:

$$\mathcal{U}(r,E) = -\mathcal{V}_V(r,E) - i\mathcal{W}_V(r,E) - i\mathcal{W}_D(r,E) + \mathcal{V}_{SO}(r,E).\mathbf{l}.\sigma + i\mathcal{W}_{SO}(r,E).\mathbf{l}.\sigma$$

$$\begin{aligned}
\mathcal{V}_V(r,E) &= V_V(E) f(r, R_V, a_V), \\
\mathcal{W}_V(r,E) &= W_V(E) f(r, R_V, a_V), \\
\mathcal{W}_D(r,E) &= -4a_D W_D(E) \frac{d}{dr} f(r, R_D, a_D), \\
\mathcal{V}_{SO}(r,E) &= V_{SO}(E) \left(\frac{\hbar}{m_\pi c}\right)^2 \frac{1}{r}\frac{d}{dr} f(r, R_{SO}, a_{SO}), \\
\mathcal{W}_{SO}(r,E) &= W_{SO}(E) \left(\frac{\hbar}{m_\pi c}\right)^2 \frac{1}{r}\frac{d}{dr} f(r, R_{SO}, a_{SO}).
\end{aligned}$$

The form factor is a Woods-Saxon shape:

$$f(r, R_i, a_i) = (1 + \exp[(r - R_i)/a_i])^{-1} ,$$

Annex: Models for direct processes

1. Distorted Wave Born Approximation (DWBA)

- Scattering and absorption are the main processes
- Any reaction channel does not have prevailing contribution to the total cross section.

2. Coupled channels method (CC)

- Full consideration of several selected reaction channels
- The influence of the discarded channels is taken into account through the optical potential of the nucleus

In case of spherical optical potential: $R_i = r_i A^{1/3}$

In case of rotational model with static deformation:

$$R_i = r_i A^{1/3}\left[1 + \sum_{\lambda=2,4,\dots} \beta_\lambda Y_\lambda^0(\Omega)\right],$$

Y — spherical harmonics,
β_2 — quadrupole deformation of the nucleus

In case of vibrational model with dynamic deformation:

$$R_i = r_i A^{1/3}\left[1 + \sum_{\lambda\mu} \alpha_{\lambda\mu} Y_\lambda^\mu(\Omega)\right],$$